Computer Networks 112 (2017) 84–94

Contents lists available at ScienceDirect

Computer Networks

journal homepage: www.elsevier.com/locate/comnet

Time-efficient cooperative spectrum sensing via analog computation over multiple-access channel

Meng Zheng[a,1,*], Chi Xu[a,b], Wei Liang[a,*], Haibin Yu[a,*], Lin Chen[c]

[a] Key Laboratory of Networked Control Systems, Chinese Academy of Sciences, and with State Key Laboratory of Robotics, Shenyang Institute of Automation, Chinese Academy of Sciences, 110016 Shenyang, China
[b] University of Chinese Academy of Sciences, 100039 Beijing, China
[c] Laboratoire de Recherche en Informatique (LRI), University of Paris-Sud XI, 91405 Orsay, France

ARTICLE INFO

Article history:
Received 15 January 2016
Revised 31 August 2016
Accepted 29 October 2016
Available online 1 November 2016

Keywords:
Cognitive radio
Spectrum sensing
Energy detection
Multiple-access channel
Analog computation

ABSTRACT

Conventional cooperative spectrum sensing (CSS) schemes in cognitive radio networks (CRNs) require that the secondary users (SUs) report their sensing data separately in the time domain to the fusion center, which yields long reporting delay especially in the case of large number of cooperative SUs. By exploiting the computation over multiple-access channel (CoMAC) method, this paper proposes a novel CoMAC-based CSS scheme that allows the cooperative SUs to encode their local statistics in transmit power and to transmit simultaneously the modulated symbols sequence carrying transmit power information to the fusion center. The fusion center then makes the final decision on the presence of primary users by recovering the overall test statistic of energy detection from the energy of the received signal. Performance metrics of the CoMAC-based CSS scheme, i.e., detection probability and false alarm probability, are further derived based on the central limit theorem. Finally, based on the derived detection and false alarm probabilities, both energy detection threshold and spectrum sensing time are optimized to improve the average throughput of the CRN. Simulations demonstrate the efficiency of this work.

1. Introduction

With the proliferation of wireless technologies, spectrum scarcity problem hinders the further development of nowadays wireless communication systems. However, it was reported that most of the currently allocated spectrums were mainly underuitlized by licensed primary users (PUs) [2]. For this, an emerging technology-cognitive radio (CR), with which the secondary users (SUs) are able to detect the spectrum opportunity and access the vacant spectrum in an opportunistic way, has received much attention recently [3–6].

Spectrum sensing functions have been frequently considered as important components in existing CR approaches, such as [7–10]. However, due to the presence of noise and fading of wireless channels, hidden terminals, obstacles and so on, spectrum sensing of individual nodes cannot achieve high detection accuracies. In contrast, cooperative spectrum sensing (CSS) exploits a parallel fusion sensing architecture in which independent SUs transmit their sensing data to a fusion center. The fusion center then makes a final soft or hard decision regarding the presence or absence of PUs [11,12]. The cooperative gains in spectrum sensing performance have been extensively demonstrated in existing works [13–25].

In conventional CSS schemes, the local statistic of each SU basically has to be sent to the fusion center in different time slots based on a time division multiple access (TDMA) scheme [13–23] or a random access scheme [24,25], due to the extremely limited bandwidth of the common control channel.[2] Correspondingly, the fusion center decodes each received local statistic separately and finally computes the overall test statistic which in this paper turns out the weighted arithmetic mean of the collected local statistics. The drawback of conventional CSS schemes [26,27] is the large reporting delay, especially when the CRN scales. Code division multiple access (CDMA) and orthogonal frequency division multiple access (OFDMA) can allow SUs to transmit concurrently in the same time slot their local statistics to the fusion center. How-

* Corresponding authors.
E-mail addresses: zhengmeng_6@sia.cn (M. Zheng), xuchi@sia.cn (C. Xu), weiliang@sia.cn (W. Liang), yhb@sia.cn (H. Yu), Lin.Chen@lri.fr (L. Chen).

[1] Parts of this paper were presented at the IEEE Conference on Communications-the 7th Workshop on Cooperative and Cognitive Networks (CoCoNet7), London, UK, June 2015 [1].

[2] Notice that, in some cases, e.g. [12], a dedicated control channel is not mandatory for reporting the sensing results in the conventional CSS schemes.

http://dx.doi.org/10.1016/j.comnet.2016.10.015
1389-1286/

ever, either CDMA or OFDMA requires a reporting control channel with large bandwidth, which is impractical in the CRN scenario.

Motivated by the recent robust analog function computation scheme–computation over multiple-access channel (CoMAC) [28], this paper proposes a novel CoMAC-based CSS scheme, in which each SU first transmits a distinct complex-valued sequence at a transmit power depending on the SU reading and consequently the received energy at the fusion center equals the sum of all transmit energies corrupted by background Gaussian noise. The fusion center then takes advantage of the collected energy information to estimate the desired weighted arithmetic mean of the local statistics from SUs, based on which the spectrum availability is determined. This paper then establishes an analytical framework on the performance of the proposed CoMAC-based CSS scheme. The major contributions of this paper are summarized as follows:

- We develop a CoMAC-based CSS scheme to accelerate the spectrum sensing in CRNs with guaranteed sensing accuracy. The proposed CSS scheme allows each SU to concurrently transmit a large sequence of modulated symbols to the fusion center, with the magnitude of each symbol carrying the information of its weighted local statistic and the pre-compensation for the reporting channel magnitude. With the superposition property of wireless channels, the fusion center could recover the global statistic from the received signal energy. In contrast to conventional CSS schemes, the CoMAC-based CSS scheme needs only *one reporting time unit* to collect all of the local statistics.
- Based on the central limit theorem, we prove that the distribution of the received signal energy at the fusion center can be approximated by a Gaussian distribution. Then, we derive the detection probability and the false alarm probability, two primary performance metrics of the proposed CSS scheme, and show their asymptotic trends.
- We further optimize the throughput performance of the CoMAC-based CSS scheme via formulating an optimization problem in terms of spectrum sensing time and detection threshold.
- Simulation results demonstrate the high approximation accuracy of the CoMAC-based CSS scheme and show that the proposed CSS scheme could yield much higher average throughput than conventional CSS schemes while guaranteeing almost the same sensing performance.

The rest of this paper is organized as follows. Section 2 reviews the related work of this paper. In Section 3, the system model and conventional CSS schemes are briefly introduced. In Section 4, the proposed CoMAC-based CSS scheme is particularly illustrated. In Section 5 sensing performance of the proposed CoMAC-based CSS scheme is approximated. In Section 6, both the energy detection threshold and the spectrum sensing time are optimized to improve the average throughput of the CRN. In Section 7, simulations are employed to validate the efficiency of the proposed CSS scheme. Finally, we draw conclusions in Section 8.

2. Related work

In the context of CSS in CRNs, the optimal voting rule and energy detection threshold for minimizing the total sensing error rate, and the least number of CRs fulfilling the targeted error rate constraints under hard decision were derived in [13]. The optimal number of SUs in CSS for lognormal shadowing channels, static additive white gaussian noise channels and Rayleigh fading channels when considering the efficiency of resources usage in the system design was derived in [14]. Unlike the works [13,14] optimizing the number of sensing SUs, reference [15] studied throughput optimization of the hard fusion based sensing using the "*K*-out-of-*N*" rule for energy-constrained CRNs. Reference [16] focused on the performance analysis and comparison of hard decision and soft decision based CSS schemes in the presence of reporting channel errors. Reference [17] proposed an algorithm for a quantization-based CSS scheme in CRNs, which simultaneously optimizes the number of sensing samples at a local node, the number of bits for quantizing local sensing data and the global threshold at a fusion center. Different from the fundamental topics in CSS schemes [13–17], reference [18] presented a cooperative sequential detection scheme to reduce the average reporting load that is required to reach a detection decision. Sequential CSS schemes in time varying channels were investigated in [19]. Based on the past local observations from previous sensing slots, a fixed or an adaptive number of past observations were combined with the current energy values to improve the detection performance of the energy detection. Censoring is another promising method to reduce the reporting SUs since one SU does not report its sensing report unless it lies outside the a specific range. A censoring-based CSS scheme for cognitive sensor networks was proposed in [20]. The censoring thresholds to minimize the energy consumption while considering the constraints on the detection accuracy were optimized. Reference [21] generalized [20] via combining censoring and truncated sequential sensing to further reduce the reporting time of the CSS scheme. A novel objection-based CSS scheme, which includes that one of the SUs broadcasts its local decision and other SUs agree or object with the announced decision, was presented in [22]. Each objecting SU sends an objection report to the fusion center, while the agreeing SUs stay silent on their time slots. Reference [23] formulated a generalized modeling approach for sensing data with an arbitrary abnormal component and proposed a robust spectrum sensing scheme by developing a data cleansing framework. Different from the above works [13–21,23] based on TDMA reporting, reference [24] applied quickest detection in spectrum sensing in CRNs when multiple SUs collaborate with limited communication time slots and proposed a threshold random broadcast scheme without an explicit coordination for the information exchange. A random access-based reporting order control scheme for cooperative sensing was proposed in [25]. By controlling the reporting order of local statistics, the global statistic at the fusion center accumulates faster than the case without order control. More related works can be found in the recent surveys on CSS [26,27].

We observe that the local statistic transmission and the overall test statistic computation in conventional CSS schemes (under both soft decision and hard decision) are separate in the time domain. Such separation-based computation schemes are generally inefficient as a complete reconstruction of individual local statistics at the fusion center is unnecessary to compute the overall test statistic. In contrast, this paper proposes to merge the process of local statistics transmission and test statistic computation via exploiting the CoMAC scheme, which takes only one time unit of the reporting phase. With the high bandwidth efficiency, the proposed CoMAC-based CSS scheme yields higher average network throughput in comparison to conventional CSS schemes.

Note that, there are recent works which also could reduce the reporting time of CSS schemes by OFDM subcarrier modulation [29] or BPSK modulation with the same carrier frequency [30,31]. On one hand, reference [29] suffered hardware limitations on OFDM physical layer and one extra half-duplex antenna with self-cancelation technique for each SU, whereas all of these hardware limitations can be avoided in this paper. On the other hand, the works [30,31] are hard decision-based CSS schemes whose spectrum sensing performances are degraded by quantization errors, while the proposed CoMAC-based CSS scheme is immune to quantization errors since CoMAC is an analog function computation scheme. We have shown that this work could guarantee almost the same sensing performance of conventional CSS schemes by choosing a sufficiently large sequence length.

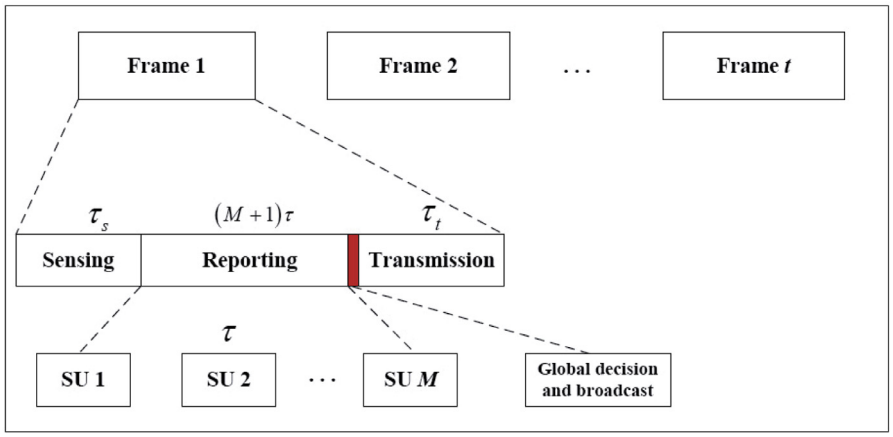

Fig. 1. The time frame architecture for the periodic spectrum sensing.

CoMAC is an enabling technique of the proposed CSS scheme. This paper computes the global statistic by following the routine of CoMAC. Although the CoMAC [28] was successfully applied to accelerate the converging speed of consensus algorithms in wireless sensor networks [32,33], to the best of our knowledge, the conference version of this paper [1] is the first one that proposes to combine CoMAC with CSS schemes in CRNs to reduce the long delay in the reporting phase of CSS schemes. Despite few contributions in CoMAC itself, this paper explores the use of CoMAC in the field of CSS schemes, innovatively analyzes and optimizes the spectrum sensing performance of the proposed CSS scheme.

3. Technical background on cooperative spectrum sensing

We consider a single-hop infrastructure CRN with M SUs, one fusion center, one control channel and one licensed channel with bandwidth W Hz. The time is divided into frames and all nodes are synchronized with the fusion center.[3] Each frame is designed with the periodic spectrum sensing for the CRN. Fig. 1 shows that the frame structure consists of three phases: a sensing phase, a reporting phase and a transmission phase. In the sensing phase, all cooperative SUs perform spectrum sensing via energy detection. In the reporting phase, the local sensing data at each SU is sequentially reported to the fusion center. Then, the fusion center makes the global decision with respect to the received local sensing results according to a given CSS fusion rule and broadcasts the global decision over the control channel at the end of the reporting phase. The time for decision fusion and broadcast at the fusion center is fixed and we set the time as one reporting time unit (or mini-slot) for simplicity in the following analysis. In the transmission phase, the transmissions of SUs are scheduled by a TDMA-MAC protocol if the PU is detected absent by the end of the reporting phase. Let τ_s and τ_t denote the lengths of the sensing phase and the transmission phase, respectively, and let τ denote one mini-slot length in the reporting phase. Then one frame length is given by $T = \tau_s + (M+1)\tau + \tau_t$. The state of PU, i.e., absent or present, does not change within one time frame. For notational convenience, we drop the time index and consider an arbitrary frame.

During the sensing phase in Fig. 1, with an analog to digital converter (ADC) each SU samples the filtered received signal by a band-pass filter (BPF). The local spectrum sensing problem at each SU, say i ($1 \le i \le M$), can be formulated as a binary hypothesis between the following two hypothesis:

$$\begin{cases} \mathcal{H}_0 : y_i(n) = u_i(n), \ n = 1, 2, \ldots, N_i \\ \mathcal{H}_1 : y_i(n) = h_i s(n) + u_i(n), \ n = 1, 2, \ldots, N_i \end{cases} \tag{1}$$

where $\mathcal{H}_0$ and $\mathcal{H}_1$ denote the PU is absent and present on the licensed channel, respectively. $N_i = \tau_s f_i^s$ denotes the number of samples, where f_i^s represents the sampling frequency of SU i. $y_i(n)$ represents the received signal at the SU i. The primary signal $s(n)$ is an independent and identically distributed random process with mean zero and variance σ_s^2. $u_i(n)$ represents the circular symmetric complex Gaussian noise with mean 0 and variance σ_u^2. Similar to [11], the channel gain $|h_i(n)|$ is assumed Rayleigh-distributed with the same variance σ_h^2. Assume that $s(n)$, $u_i(n)$, and $h_i(n)$ are independent of each other, and the average received SNR at each sensor is given as $\gamma = \frac{\sigma_h^2 \sigma_s^2}{\sigma_u^2}$. For spectrum sensing, SU i then uses the average of energy content in received samples as the test statistic for energy detector, which is given by

$$\psi_i = \frac{1}{N_i} \sum_{n=1}^{N_i} |y_i(n)|^2, \tag{2}$$

and then the local statistic of SU i, $T_i = w_i \psi_i$ $(i = 1, 2, \ldots, M)$, are reported to the fusion center, where $w_i \ge 0$ is the weighting factor associated with SU i. Without loss of generality, we assume $\sum_{i=1}^{M} w_i = 1$.

At the fusion center, the overall test statistic for spectrum sensing is calculated as

$$T_s^{all} = \sum_{i=1}^{M} T_i. \tag{3}$$

To make the final decision, the fusion center compares T_s^{all} with a threshold ε_s. The PU is estimated to be absent if $T_s^{all} < \varepsilon_s$, or present otherwise. This process is referred to as the soft decision-based CSS.

For reporting T_i to the fusion center, soft decision usually requires a reporting channel with large bandwidth. Unlike in soft decision, in hard decision, the SUs send only their binary decision results to the fusion center. The local binary decision μ_i for SU i is made as follows:

$$\mu_i = \begin{cases} 1, \ \psi_i \ge \varepsilon_i \ \text{(Presence of PUs)} \\ 0, \ \text{otherwise (Absence of PUs)} \end{cases} \tag{4}$$

where ε_i denotes the local detection threshold of SU i. At the fusion center, the overall test statistic for spectrum sensing with

[3] As the studied CRN is fully centralized, all nodes synchronize to the fusion center when they join the network. After the joining process, the synchronization among all nodes can be achieved from the periodic broadcast of global decision by the fusion center.

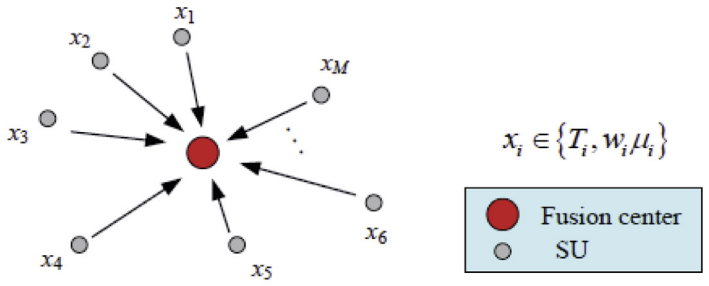

(a) An example of one single-hop CRN

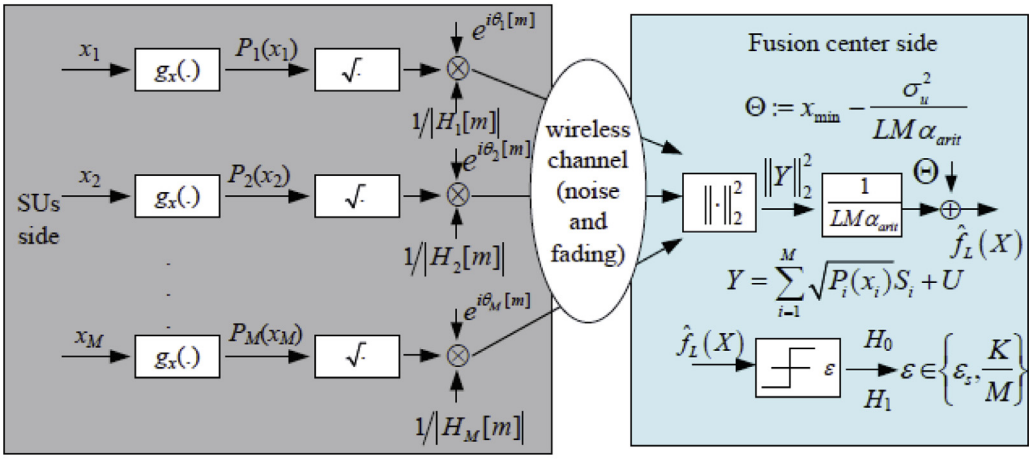

(b) Block diagram of the CoMAC-based CSS scheme

Fig. 2. Illustration on the CoMAC-based CSS scheme.

the hard decision rule is calculated as

$$T_h^{all} = \sum_{i=1}^{M} w_i \mu_i. \tag{5}$$

One of the great challenges of implementing spectrum sensing is the hidden terminal problem, which occurs when the CR is shadowed, in severe fading or inside buildings with high penetration loss, while a PU is operating in the vicinity. In order to deal with the hidden terminal problem, the decision fusion of multiple CRs can help greatly improve the spectrum sensing performance. The fusion rule adopted by fusion center is commonly termed as the K-out-of-M rule, where the final decision $\mu = 1$ if $T_h^{all} \geq \frac{K}{M}$. There are different ways of setting K. The readers will find the Chair-Varshney rule, logic-OR, logic-AND, Majority for hard decision in [7, Section VI.B].

4. CoMAC-based cooperative spectrum sensing

From Section 3, we observe that in order to compute the overall test statistic (no matter T_s^{all} in (3) or T_h^{all} in (5)), the fusion center has to collect the reports from SUs successively. This paper combines the CoMAC method [28] with conventional CSS schemes to reduce the reporting delay in the reporting phase, which finally enhances the average throughput of the CRN.

As shown in Fig. 2(a), in the CoMAC-based CSS scheme, SU i (i=1, 2, ..., M) and T_i (or $w_i\mu_i$) act as sensor i and its sensor reading x_i in the CoMAC scheme [28], respectively. In order to maintain the consistency with the formulation of the CoMAC method, we use x_i to represent the local statistic of SU i.

Fig. 2(b) illustrates the working principle of the novel CoMAC-based CSS scheme. M SUs jointly detect the presence of PUs resulting in local statistics $x_i \in \mathbb{X} \subset \mathbb{R}$, $i = 1, \ldots, M$, and send local statistics to the fusion center, where $\mathbb{X} := [x_{min}\ x_{max}]$ denotes the sensing range that is the hardware-dependent range in which the SUs are able to quantify values. The fusion center then computes an arithmetic mean of the received data.

At each SU, the local statistic is encoded in its transmit power. For this, we introduce a bijective continuous mapping $g_x : \mathbb{X} \to [0, P_{max}]$ from the set of all local statistics onto the set of all feasible transmit powers, where P_{max} represents the transmit power constraint on each SU. Note that, P_{max} depends only on the physical hardware of SUs since SUs use the common control channel (e.g., 2.4 GHz ISM band) which does not cause interferences at PUs to report local statistics. The employed mapping function is $g_x(x) = \alpha_{arit}(x - x_{min})$, where $\alpha_{arit} = \frac{P_{max}}{x_{max} - x_{min}}$. The quantity $P_i(x_i) = g_x(x_i)$ is called the transmit power of SU i. Let $S_i := (S_i[1], S_i[2], ..., S_i[L])^T \in \mathbb{C}^L$ denote a sequence of random transmit symbols independently generated by SU i and let L denote the length of the symbol sequence. Energy detection-based algorithms are generally sensitive to noise. Averaging on a large sequence of L symbols can effectively counteract the negative effect of noise on the sensing performance of the proposed CSS scheme. The symbols of the sequence are assumed to be of the form $S_i[m] = e^{\mathbf{i}\theta_i[m]}$, $m = 1, 2, \ldots, L$, where $\mathbf{i}$ denotes the imaginary unit, and $\{\theta_i[m]\}_{i,\,m}$ are continuous random phases that are independent identically and uniformly distributed on $[0,\ 2\pi)$. The assumed form of the symbol will bring convenience to the statistics calculation of the received signal [34, Appendix A]. Then the m-th transmit symbol of SU i takes the form

$$\Gamma_i[m] = \frac{\sqrt{P_i(x_i)}}{|H_i[m]|} S_i[m], \tag{6}$$

where $|H_i[m]|$ denotes the channel magnitude of an independent complex-valued flat fading process between SU i and the fusion center. We assume that the channel gain $H_i[m]$ does not change within one frame length. Therefore, we have $H_i[m] = H_i$, $m = 1, 2, \ldots, L$. It has been reported in [34] that the channel magnitude $|H_i|$ at the transmitter is sufficient to achieve the same approximation accuracy as with full channel state information H_i. Notice that. the channel inversion in (6) may lead to extremely high transmit power especially when the fading is severe. Therefore, we adopt a weighted sum of data fusion [7] by setting

$$w_i = \frac{|H_i|^2}{\sum_{i=1}^{M} |H_i|^2}. \tag{7}$$

In practical systems $\{|H_i|, w_i\}$ can be obtained by the fusion center through channel training and estimation, and together with the global decision is broadcast by the fusion center periodically. In doing so, small weights will be assigned to the SUs who suffer severe fading and their transmit powers can be significantly reduced. When $w_i = \frac{1}{M}$ $(i = 1, 2, \ldots, M)$, this work reduces to the reference [1].

Concurrent transmission of SUs yields the output at the fusion center

$$Y[m] = \sum_{i=1}^{M} \sqrt{P_i(x_i)} S_i[m] + U[m], \quad m = 1, 2, \ldots, L. \tag{8}$$

For simplicity, we reformulate (8) in a vector form

$$Y = \sum_{i=1}^{M} \sqrt{P_i(x_i)} S_i + U, \tag{9}$$

where $Y := (Y[1], Y[2], \ldots, Y[L])^T \in \mathbb{C}^L$, and $U := (U[1], U[2], \ldots, U[L])^T \in \mathbb{C}^L$ represents an independent stationary complex Gaussian noise, that is $U \sim \mathrm{CN}(\mathbf{0}, \sigma_u^2 \mathbf{I}_L)$. For simplicity, let $X = [x_1, x_2, \ldots, x_M] \in \mathbb{R}^M$ denote the local statistic vector.

Without loss of generality, we assume $w_i = \frac{1}{M}$ $(i = 1, 2, \ldots, M)$ for notational convenience in the rest of this paper. By estimating the energy of signal (9), i.e., $\|Y\|_2^2$, the following lemma gives us an estimate of the desired function arithmetic mean.

Lemma 1 *[28]. Let $f : \mathbb{R}^M \to \mathbb{R}$ be the desired function arithmetic mean, i.e., $f(X) = \frac{\sum_{i=1}^{M} x_i}{M}$. Then, given $L \in \mathbb{N}$, the unbiased and consistent estimate $\hat{f}_L(X)$ of $f(X)$ is defined to be*

$$\hat{f}_L(X) := \frac{1}{M\alpha_{arit}} \left(\frac{\|Y\|_2^2}{L} - \sigma_u^2 \right) + x_{min}. \tag{10}$$

It is reasonable to assume that all CSS parameters in (10) including α_{arit}, x_{min}, L and σ_u^2 are known to the fusion center. α_{arit} and x_{min}, both of which are hardware-dependent parameters, are reported by the SUs to the fusion center before the CSS process. L is a global CSS parameter which is determined by the fusion center. σ_u^2 can be estimated according to the long-term historical observation at the fusion center.

With Lemma 1, the fusion center achieves the estimate of T_s^{all} in (3) (or T_h^{all} in (5)), denoted by $\hat{f}_L(\mathbf{T})$, where $\mathbf{T} = [T_1, T_2, \ldots, T_M] \in \mathbb{R}^M$. Instead of T_s^{all} (or T_h^{all}), $\hat{f}_L(\mathbf{T})$ is then exploited by the fusion center to perform energy detection. From (6), we know that CoMAC is an analog computation scheme with amplitude modulation at the SUs side. In addition, T_s^{all} is more informative than T_h^{all} for the fusion center to make the global decision. Therefore, for the CoMAC-based CSS scheme, soft decision does not need extra bandwidth but enjoys higher sensing performance in comparison to hard decision. In the rest of this paper, we will only focus on the sensing performance analysis and optimization for the CoMAC-based CSS scheme with soft decision.

5. Sensing performance analysis

Detection probability and false alarm probability are two main performance metrics measuring the sensing performance of spectrum sensing in CRNs. Detection probability, P_d, is the probability that if there are PU activities, the SUs can detect them successfully. While false alarm probability, P_f, is the probability that if there are no PU activities, the SUs falsely estimate that the PUs are present. Therefore, P_d and P_f of the proposed CoMAC-based CSS scheme are given by

$$P_d = \Pr\left(\hat{f}_L(\mathbf{T}) \geq \varepsilon_s | \mathcal{H}_1 \right) \tag{11}$$

and

$$P_f = \Pr\left(\hat{f}_L(\mathbf{T}) \geq \varepsilon_s | \mathcal{H}_0 \right). \tag{12}$$

According to Lemma 1, the detection condition in (11) and (12) can be reformulated as follows

$$\hat{f}_L(\mathbf{T}) \geq \varepsilon_s \Leftrightarrow \|Y\|_2^2 \geq \eta(\varepsilon_s; L, M), \tag{13}$$

where $\eta(\varepsilon_s; L, M) := LM\alpha_{arit}(\varepsilon_s - x_{min}) + L\sigma_u^2$.

5.1. Approximation of sensing performances

From Lemma 1, we know that the sum-energy of vector Y (i.e., $\|Y\|_2^2$) is critical for the estimation of function $f(\mathbf{T})$. Thus we first give out the expression of $\|Y\|_2^2$

$$\|Y\|_2^2 = \Delta_1 + \Delta_2 \tag{14}$$

where $\Delta_1 = \sum_{i=1}^{M} P_i(T_i)$ and $\Delta_2 = U^H U + \sum_{i=1}^{M} \sum_{j=1, j\neq i}^{M} \sqrt{P_i(T_i) P_j(T_j)} S_i^H S_j + 2 \sum_{i=1}^{M} \sqrt{P_i(T_i)} \mathrm{Re}\{S_i^H U\}$.

Apparently, Δ_1 is a linear combination of all T_i, $i = 1, 2, \ldots, M$. According to (2), the mean and the variance of T_i are given by

$$\mathbb{E}\{T_i\} = \begin{cases} \sigma_u^2, & \mathcal{H}_0 \\ (\gamma + 1)\sigma_u^2, & \mathcal{H}_1 \end{cases} \tag{15}$$

$$\mathbb{V}ar\{T_i\} = \begin{cases} \frac{\sigma_u^4}{N_i}, & \mathcal{H}_0 \\ \frac{(2\gamma+1)}{N_i}\sigma_u^4, & \mathcal{H}_1 \end{cases} \tag{16}$$

For convenience, we let $N_i = N = 2\tau_s W$ (i.e., $f_i^s = 2W$) in the rest of this paper.

According to (2), we know that T_i is the weighted sum of $|y_i(n)|^2$, each of which is the square function of $(h_i s(n) + u_i(n))$, where h_i and u_i are previously assumed mutually independent Rayleigh and Gaussian distributed variables, respectively. As the locations of the SUs are different, it is reasonable to assume that (h_i, u_i) and (h_j, u_j) (or equivalently, y_i and y_j) are independent, which further implies the independence of T_i. Then, the mean and the variance of Δ_1 can be trivially calculated as follows

$$\mathbb{E}\{\Delta_1\} = L \sum_{i=1}^{M} \mathbb{E}\{P_i(T_i)\} = \begin{cases} L\Omega_0, & \mathcal{H}_0 \\ L\Omega_1, & \mathcal{H}_1 \end{cases} \tag{17}$$

$$\mathbb{V}ar\{\Delta_1\} = L^2 \sum_{i=1}^{M} \mathbb{V}ar\{P_i(T_i)\} = \begin{cases} \frac{L^2 M \alpha_{arit}^2 \sigma_u^4}{N}, & \mathcal{H}_0 \\ \frac{L^2 M \alpha_{arit}^2 \sigma_u^4 (2\gamma+1)}{N}, & \mathcal{H}_1 \end{cases} \tag{18}$$

where for brevity we define $\Omega_0 := M\alpha_{arit}\left(\sigma_u^2 - x_{min}\right)$ and $\Omega_1 := M\alpha_{arit}\left((\gamma + 1)\sigma_u^2 - x_{min}\right)$.

Similar to [28], we can also calculate the mean and variance of Δ_2 as follows

$$\mathbb{E}\{\Delta_2\} = L\sigma_u^2 \tag{19}$$

$$\begin{aligned}\mathbb{V}ar\{\Delta_2\} =& L\sum_{i=1}^{M}\sum_{j\neq i}^{M}\sqrt{\mathbb{E}\{P_i(T_i)P_j(T_j)\}} + L\sigma_u^4 \\ &+ 2L\sigma_u^2\sum_{i=1}^{M}\mathbb{E}\{P_i(T_i)\} \\ \hat{=}& \begin{cases} L\Omega_0(M-1+2\sigma_u^2), & \mathcal{H}_0 \\ L\Omega_1\left(M-1+2\sigma_u^2\right)+L\sigma_u^4, & \mathcal{H}_1 \end{cases}\end{aligned} \tag{20}$$

where "$\hat{=}$" follows from $\mathbb{E}\{P_i(T_i)P_j(T_j)\} = \mathbb{E}\{P_i(T_i)\}\mathbb{E}\{P_j(T_j)\}$, for $i \neq j$.

Lemma 2. *$\mathbb{E}\{\Delta_1\Delta_2\} = \mathbb{E}\{\Delta_1\}\mathbb{E}\{\Delta_2\}$ holds for the joint probability distribution of* $\mathbf{T}$.

The proof of Lemma 2 will be given in Appendix A.

With Lemma 2 and (17)–(20) in hand, we can easily calculate the mean and the variance of $\|Y\|_2^2$

$$\mathbb{E}\{\|Y\|_2^2\} = \begin{cases} L(\Omega_0+\sigma_u^2), & \mathcal{H}_0 \\ L(\Omega_1+\sigma_u^2), & \mathcal{H}_1 \end{cases} \tag{21}$$

$$\mathbb{V}ar\{\|Y\|_2^2\} = \begin{cases} L\Omega_0(M-1+2\sigma_u^2) + \frac{L^2M\alpha_{arit}^2\sigma_u^4}{N}, & \mathcal{H}_0 \\ L\Omega_1(M-1+2\sigma_u^2) + L\sigma_u^4 & \\ \quad + \frac{L^2M\alpha_{arit}^2\sigma_u^4(2\gamma+1)}{N}, & \mathcal{H}_1 \end{cases} \tag{22}$$

The expression of $\|Y\|_2^2$ is so complicated that its exact distribution is unavailable, even if the mean and the variance of $\|Y\|_2^2$ are known. However, with the aid of the central limit theorem [35], we can approximate the distribution of $\|Y\|_2^2$ by Gaussian distribution.

Theorem 1. *For any fixed M, $P_{max} < \infty$ and a compact set $\mathbb{X}$, we have*

$$\forall\ T(y) \in \mathbb{X}^M : \frac{\|Y\|_2^2 - \mathbb{E}\{\|Y\|_2^2\}}{\sqrt{\mathbb{V}ar\{\|Y\|_2^2\}}} \xrightarrow{d} \mathrm{N}(0,1), \tag{23}$$

as $L \to \infty$, where $\xrightarrow{d}$ denotes the convergence in distribution.

The proof of Theorem 1 will be given in Appendix B.

Considering (11) and Theorem 1, we know that for a sufficiently large L, P_f finds a well-qualified approximation $\tilde{P}_f$ as follows

$$\begin{aligned} P_f &= \Pr(\|Y\|_2^2 \geq \eta(\varepsilon_s; L, M)|\mathcal{H}_0) \\ &\approx Q\left(\frac{\eta(\varepsilon_s; L, M) - L(\Omega_0+\sigma_u^2)}{\sqrt{L\Omega_0(M-1+2\sigma_u^2) + \frac{L^2M\sigma_u^4\alpha_{arit}^2}{N}}}\right) \\ &= Q\left(\frac{LM\alpha_{arit}\left(\varepsilon_s - \sigma_u^2\right)}{\sqrt{L\Omega_0(M-1+2\sigma_u^2) + \frac{L^2M\sigma_u^4\alpha_{arit}^2}{N}}}\right) \\ &= \tilde{P}_f, \end{aligned} \tag{24}$$

where "$\approx$ " straightforwardly follows from Theorem 1. $Q(x)$ is the complementary distribution of the standard Gaussian, i.e.,

$$Q(x) = \frac{1}{\sqrt{2\pi}}\int_x^\infty \exp\left(-\frac{t^2}{2}\right)dt.$$

Similarly, the approximation of P_d for the sufficiently large L, $\tilde{P}_d$, is given by

$$\tilde{P}_d = Q\left(\frac{LM\alpha_{arit}\left(\varepsilon_s - (1+\gamma)\sigma_u^2\right)}{\sqrt{L\Omega_1(M-1+2\sigma_u^2) + L\sigma_u^4 + \frac{L^2M\alpha_{arit}^2\sigma_u^4(2\gamma+1)}{N}}}\right). \tag{25}$$

From (24) and (25), we have to constrain ε_s to the domain $\sigma_u^2 < \varepsilon_s < (1+\gamma)\sigma_u^2$ in order to make $\tilde{P}_d > 0.5$ and $\tilde{P}_f < 0.5$, which should be the case for most CR scenarios.

Remark 1. It is obvious in (24) and (25) that the detection performance in terms of $\tilde{P}_d$ and $\tilde{P}_f$ under the CoMAC-CSS scheme does not only depend on $\{\tau_s, \varepsilon_s\}$ (or $\{N, \varepsilon_s\}$), but also depends on the sequence length L. For $\sigma_u^2 < \varepsilon_s < (1+\gamma)\sigma_u^2$, we conclude that $\tilde{P}_f$ and $\tilde{P}_d$ are monotonically decreasing and increasing in L, respectively. As $L \to \infty$, we find a lower bound of $\tilde{P}_f$, given by $Q(\sqrt{MN}(\frac{\varepsilon_s}{\sigma_u^2} - 1))$, and an upper bound of $\tilde{P}_d$, given by $Q(\sqrt{\frac{MN}{2\gamma+1}}(\frac{\varepsilon_s}{\sigma_u^2} - (1+\gamma)))$.

5.2. Analysis of approximation error

From the definition of T_s^{all} in (3), we know that T_s^{all} is simply the average of the squares sum of MN Gaussian variables, each with mean 0 and variance σ_u^2. Hence, normalized with σ_u^2 (or $\sigma_u^2(1+\gamma)$), T_s^{all} has a central Chi-square distribution with MN degrees of freedom [8]

$$\begin{aligned}\mathcal{H}_0:\ \frac{MN}{\sigma_u^2}T_s^{all} &= \sum_{i=1}^{M}\sum_{n=1}^{N}\left(\frac{|u_i(n)|}{\sigma_u}\right)^2 \\ &= \sum_{i=1}^{M}\sum_{n=1}^{N}\left(z_i^{(0)}(n)\right)^2 \\ &\sim \chi_{MN}^2\end{aligned} \tag{26}$$

and

$$\begin{aligned}\mathcal{H}_1:\ \frac{MN}{\sigma_u^2(1+\gamma)}T_s^{all} &= \sum_{i=1}^{M}\sum_{n=1}^{N}\left(\frac{|h_is(n)+u_i(n)|}{\sigma_u\sqrt{1+\gamma}}\right)^2 \\ &= \sum_{i=1}^{M}\sum_{n=1}^{N}\left(z_i^{(1)}(n)\right)^2 \\ &\sim \chi_{MN}^2,\end{aligned} \tag{27}$$

where $z_i^{(0)}(n) \sim \mathrm{N}(0,1)$ and $z_i^{(1)}(n) \sim \mathrm{N}(0,1)$.

Then the detection probability and the false alarm probability of conventional CSS schemes are given by

$$\begin{aligned}\check{P}_d &= \Pr\left(T_s^{all} \geq \varepsilon_s|\mathcal{H}_1\right) \\ &= Q_{\chi_{MN}^2}\left(\frac{MN}{\sigma_u^2(1+\gamma)}\varepsilon_s\right) \\ &= \frac{\Gamma\left(\frac{MN}{2}, \frac{MN\varepsilon_s}{2\sigma_u^2(1+\gamma)}\right)}{\Gamma\left(\frac{MN}{2}\right)}\end{aligned} \tag{28}$$

and

$$\begin{aligned}\check{P}_f &= \Pr\left(T_s^{all} \geq \varepsilon_s|\mathcal{H}_0\right) \\ &= Q_{\chi_{MN}^2}\left(\frac{MN}{\sigma_u^2}\varepsilon_s\right) \\ &= \frac{\Gamma\left(\frac{MN}{2}, \frac{MN\varepsilon_s}{2\sigma_u^2}\right)}{\Gamma\left(\frac{MN}{2}\right)},\end{aligned} \tag{29}$$

where $Q_{\chi_{MN}^2}(x)$ denotes the right-tail probability at x for a χ_{MN}^2 random variable. $\Gamma(x)$ is the gamma function, i.e., $\Gamma(x) = \int_0^\infty t^{x-1}\exp(-t)dt$, and $\Gamma(x, a)$ is the incomplete gamma function, i.e., $\Gamma(x,a) = \int_a^\infty t^{x-1}\exp(-t)dt$.

Now we are ready to derive the closed-form error expressions of the proposed CoMAC-based CSS scheme, in terms of sensing performances. Let e_d and e_f represent the approximation errors of the detection probability and the false alarm probability of the proposed CoMAC-based CSS scheme, respectively

$$e_d = \check{P}_d - \tilde{P}_d \tag{30}$$

and

$$e_f = \check{P}_f - \tilde{P}_f. \tag{31}$$

Then, the approximation error of the probability of the false-decision made by the fusion center is given by

$$e_{fd} = \Pr(\mathcal{H}_0)e_f + \Pr(\mathcal{H}_1)e_d. \tag{32}$$

Evident from (24), (25), (28) and (29), the expressions of e_d in (30), e_f in (31) and e_{fd} in (32) are so complicated that the sensing accuracy of the proposed CSS scheme is difficult to be validated without the aids of simulations. The demonstration of the approximation efficiency will be made through simulations in Section 7, and in the following section we use $\tilde{P}_d$ and $\tilde{P}_f$ instead of $\check{P}_d$ and $\check{P}_f$ to perform the optimization of sensing parameters.

6. Spectrum sensing optimization

The objective of the spectrum sensing optimization problem is to identify the optimal detection threshold and the spectrum sensing time such that the achievable throughput of the CRN is maximized while the PUs are sufficiently protected. Given a sufficiently large L, the optimization problem can be formulated as follow

$$\max_{\{\varepsilon_s,\tau_s\}\geq 0} F(\varepsilon_s, \tau_s) \tag{33a}$$

$$s.t.\ \tilde{P}_d(\varepsilon_s, \tau_s) \geq \omega, \tag{33b}$$

$$\tau_s \leq T - 2\tau, \tag{33c}$$

where $F(\varepsilon_s, \tau_s) = \frac{T-2\tau-\tau_s}{T}\left(1 - \tilde{P}_f(\varepsilon_s, \tau_s)\right)C_0 \Pr(\mathcal{H}_0)$ represents the average throughput of the CRN. C_0 denotes the throughput of SUs if they are allowed to continuously operate in the case of $\mathcal{H}_0$, and $\Pr(\mathcal{H}_0)$ denotes the probability of $\mathcal{H}_0$. When the PU is active, the throughput of SUs will be close to zero and thus neglected in the definition of $F(\varepsilon_s, \tau_s)$. ω is a pre-specified threshold that is close to but less than 1.

6.1. Detection threshold optimization

Lemma 3. *Suppose an optimal solution of problem (33) exists, denoted as $(\varepsilon_s^*, \tau_s^*)$, where * symbol denotes optimality. Then, we have*

$$\varepsilon_s^* = \frac{\sqrt{\mathbb{V}ar\left(\|Y\|_2^2|\mathcal{H}_1\right)}Q^{-1}(\omega) + L\Omega_1}{LM\alpha_{arit}} + x_{min}, \tag{34}$$

where $\mathbb{V}ar\left(\|Y\|_2^2|\mathcal{H}_1\right)$ is given by (22).

The proof of Lemma 3 will be given in Appendix C.

Remark 2. Expanding the expression of ε_s^* in (34), we find that ε_s^* is a monotonically decreasing function of L, i.e., $\varepsilon_s^*(L) = \sqrt{\Psi(L) + \frac{(2\gamma+1)\sigma_u^4}{MN}}Q^{-1}(\omega) + (\gamma+1)\sigma_u^2$, where $\Psi(L) := \frac{M\alpha_{arit}\left((\gamma+1)\sigma_u^2 - x_{min}\right)(M-1+2\sigma_u^2)+\sigma_u^4}{LM^2\alpha_{arit}^2}$. Obviously, as $L \to \infty$, we have

$$\hat{\varepsilon}_s^* := \lim_{L\to\infty} \varepsilon_s^*(L) = \left(\sqrt{\frac{(2\gamma+1)}{MN}}Q^{-1}(\omega) + \gamma + 1\right)\sigma_u^2,$$

where $\hat{\varepsilon}_s^*$ is the exact detection threshold for conventional CSS schemes.

Table 1
Parameter values used in the simulation.

Parameter	Value
The number of sensing SUs M	$\{5, 6, \ldots, 25\}$
The weighting factor of each SU w_i	$\frac{1}{M}$
The length of the symbol sequence L	$\{30, 31, \ldots, 500\}$
The average received SNR at each SU γ	-10 dB
The target detection probability ω	0.9
The occurrence probability of $\mathcal{H}_1$ $\Pr(\mathcal{H}_1)$	0.2
The occurrence probability of $\mathcal{H}_0$ $\Pr(\mathcal{H}_0)$	0.8
The bandwidth of the licensed band W	6 MHz
The length of one time frame T	300 ms
The length of one mini-slot τ	10 ms
The variance of noise σ_u^2	{1, 1.5, 2}
The coefficient of transmit power coding α_{arit}	10
The throughput of SUs when PUs are inactive C_0	6.6582 bits/s/Hz

6.2. Sensing time optimization

Plugging (34) into problem (33), we then achieve its equivalent form

$$\max \hat{F}(\tau_s) \tag{35a}$$

$$s.t.\ 0 \leq \tau_s \leq T - 2\tau, \tag{35b}$$

where $\hat{F}(\tau_s) = \frac{T-2\tau-\tau_s}{T}\left(1 - \tilde{P}_f(\tau_s; \varepsilon_s^*)\right)C_0 \Pr(\mathcal{H}_0)$.

Theorem 2. *When $\varepsilon_s^* \geq \sigma_u^2$ (i.e., $\tilde{P}_f \leq 0.5$), problem (35) is convex and its optimal solution is unique.*

The proof of Theorem 2 will be given in Appendix D.

Efficient solution methods, such as interior-point methods [36], could be then found to solve problem (35) in polynomial time.

7. Simulation

This section performs simulations to verify the effectiveness of the proposed CoMAC-based CSS scheme. All simulated parameters are summarized in Table 1, representing values describing typical CR and WSN scenarios, following, e.g., [7,11]. The simulation code is developed by MATLAB and all the figures in simulations are traced based on the proposed and existing results.

7.1. Approximation error analysis

For an arbitrarily chosen $\varepsilon_s \in (\sigma_u^2, (1+\gamma)\sigma_u^2)$ and $\tau_s \in (0, T - (M+1)\tau)$, say $\varepsilon_s = 1.05$ and $\tau_s = 10$ms, Fig. 3 demonstrates the approximation accuracy of the CoMAC-based CSS scheme with respect to L and M when $\sigma_u^2 = 1$. We observe that e_d, e_f and e_{fd} monotonically converge to zero as L increases to infinity, and decrease as the number of SUs M increases. This stems from the fact that larger L and M imply more summation terms in (14), which in turn improves the approximation accuracy because of the central limit theorem. Similar to Fig. 3, we also show the approximation error analysis in Fig. 4 with respect to L and σ_u^2 when $M = 10$. Fig. 4 presents that all of e_d, e_f and e_{fd} monotonically converge to zero as L increases to infinity, and increase as the noise variance σ_u^2 increases. Despite the proposed CSS scheme is shown sensitive to noise, we can still balance a large σ_u^2 by selecting a moderate L.

In order to achieve a low approximation error (e.g., $|e_d|, |e_f|, |e_{fd}| < 10^{-3}$), we should adopt a large enough L (e.g., $L \in [470, +\infty)$) from Figs. 3 and 4. Note that L cannot be arbitrarily large in one reporting mini-slot. Taking IEEE 802.11af (WiFi over TV white space) physical layer [37] whose one symbol time including cyclic prefix duration is $t_s = 4\mu$s as an example, we

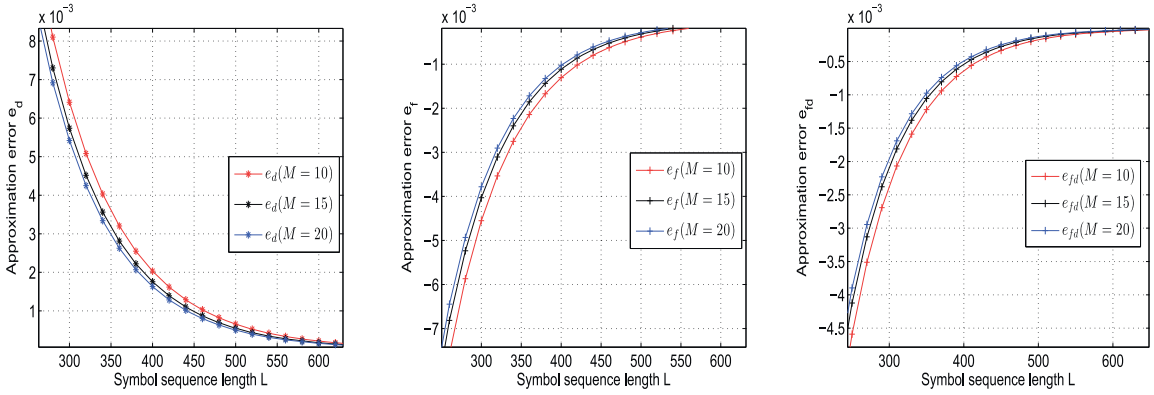

(a) The approximation error e_d (b) The approximation error e_f (c) The approximation error e_{fd}

Fig. 3. Approximation error analysis with respect to L and M ($\sigma_u^2 = 1$).

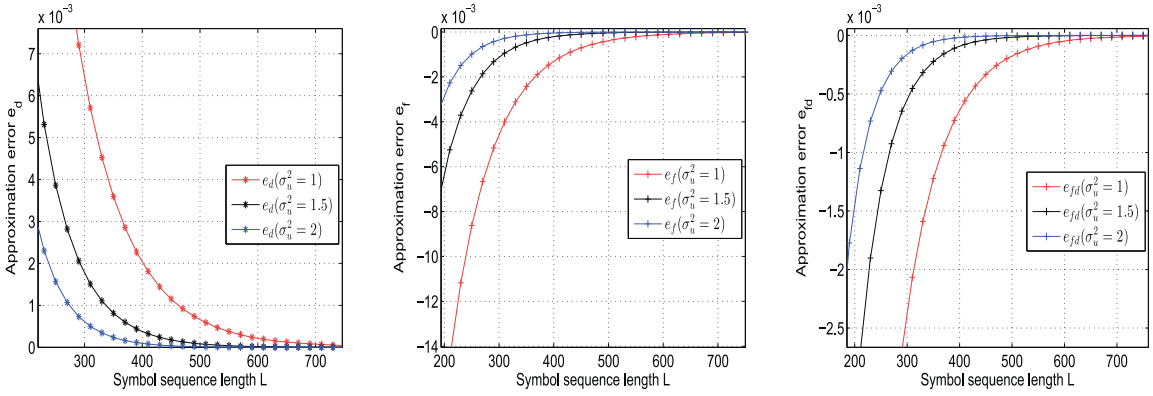

(a) The approximation error e_d (b) The approximation error e_f (c) The approximation error e_{fd}

Fig. 4. Approximation error analysis with respect to L and σ_u^2 ($M = 10$).

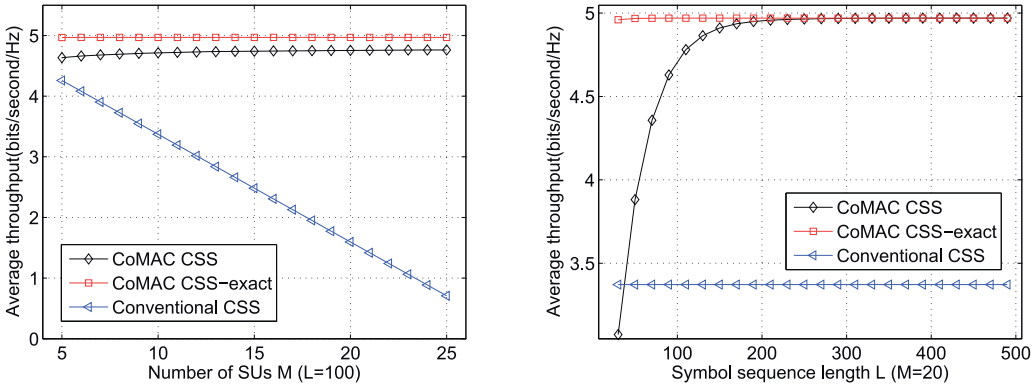

(a) Average throughput vs. M (b) Average throughput vs. L

Fig. 5. Throughput comparison between different CSS schemes.

calculate the maximum number of symbols during one reporting mini-slot by $\frac{\tau}{t_s} = 2500$ (>470), which proves that the proposed scheme is indeed feasible.

Another important observation is that, although we plotted e_d and e_f for different reasonable parameters, e_d and e_f are always positive and negative as shown in Fig. 3, respectively. This fact guarantees that the optimal solution $(\varepsilon_s^*, \tau_s^*)$ to problem (33) fulfills the protection constraint of the PU, i.e., $\check{P}_d(\varepsilon_s^*, \tau_s^*) > \tilde{P}_d(\varepsilon_s^*, \tau_s^*) = \omega$, and $F(\varepsilon_s^*, \tau_s^*)$ presents a lower bound of the maximum to problem (33) with $\check{P}_d$ and $\check{P}_f$.

7.2. Performance comparison

This subsection presents the throughput comparison of different CSS schemes. For convenience, we denote the CoMAC-based scheme with $\tilde{P}_d$, and $\tilde{P}_f$ as "CoMAC CSS", the CoMAC-based scheme

with $\check{P}_d$ and $\check{P}_f$ as "CoMAC CSS-exact", and the conventional CSS schemes with the Gaussian distribution of $\check{P}_d$ and $\check{P}_f$ [7,11,22] as "Conventional CSS".

Fig. 5(a) and (b) display how the optimal throughput evolves with parameters M and L, respectively, where M varies from 5 to 25 with fixed L ($L = 100$) and L varies from 30 to 500 with fixed M ($M = 10$).

As shown in Fig. 5(a), "Conventional CSS" degrades as M increases, which means that the cost of large reporting time dominates the performance gain owing to cooperation diversity. Conversely, both "CoMAC CSS" and "CoMAC CSS-exact" could benefit from the cooperation diversity without a large portion of time on reporting local statistics, and thus outweigh "Conventional CSS".

From Fig. 5(b), we know that by using a sufficiently large L (e.g., $L > 50$), "CoMAC CSS" dominates "Conventional CSS" even if the number of SUs is not very large ($M = 10$). The network throughput under the "Conventional CSS", 3.3717, can be boosted up to 4.9696 in the case of $L = 250$, in which the throughput gain of "CoMAC CSS" is roughly calculated $\frac{4.9696-3.3717}{3.3717} \approx 47.39\%$. Finally, due to the negligible approximation errors e_d and e_f, we observe that "CoMAC CSS" matches "CoMAC CSS-exact" very well when $L > 250$.

8. Conclusion

A novel CoMAC-based CSS scheme for CRNs has been proposed in [1]. Unlike conventional CSS schemes, the proposed CoMAC-based CSS scheme takes advantage of the CoMAC to accelerate the CSS process via merging the reporting and the computation steps of CSS, which noticeably reduces the reporting delay in conventional CSS schemes. Based on the estimation of the desired arithmetic mean function of local statistics, we analyze the detection probability and the false alarm probability of the proposed CoMAC-based CSS scheme. Finally, we obtain the optimal energy detection threshold and spectrum sensing time yielding the maximal average throughput of the CRN.

Extensive simulations have demonstrated that, using much less reporting time, the CoMAC-based CSS scheme yields almost the same sensing performance as conventional CSS schemes, provided that the symbol sequence length L is sufficiently large. In addition, for a suitably chosen L, the average throughput of the CoMAC-based CSS scheme is shown much higher than that of conventional CSS schemes, especially when the number of cooperative SUs is large.

The disadvantage of the proposed CoMAC-based CSS scheme lies in the high energy consumption when the length of the symbol sequence is large. In order to address the issue of high energy consumption, we have to formulate a completely novel optimization problem instead of problem (33) and to redesign a corresponding solution method to it as well. We will leave this interesting direction as a future work.

Acknowledgments

This work was supported by the Natural Science Foundation of China under grant (61233007, 61304263, 61673371, 71602124) and the French Agence Nationale de la Recherche (ANR) under the grant Green-Dyspan (ANR-12-IS03).

The authors are grateful to Dr. Jinsong Wu who is currently an associate professor at Department of Electrical Engineering-University of Chile for his valuable comments and discussions on some of the topics of this paper.

Appendix A. Proof of Lemma 2

Proof. Due to the fact that the local statistic $\mathbf{T}$, the modulated symbol sequence S_i, $i = 1, \ldots, M$, and the noise U are mutually independent, $\mathbb{E}\{\Delta_1\Delta_2\}$ is calculated as follows

$$\begin{aligned}\mathbb{E}\{\Delta_1\Delta_2\} =& \mathbb{E}\{\Delta_1 U^H U\} + \mathbb{E}\{\Delta_1\big(\Delta_2 - U^H U\big)\}\\ \cong& \mathbb{E}\{\Delta_1 U^H U\}\\ =& \mathbb{E}\{\Delta_1\}\mathbb{E}\{U^H U\}\\ =& \mathbb{E}\{\Delta_1\}\mathbb{E}\{\Delta_2\},\end{aligned}$$

where "$\cong$" follows from [28, Lemma 1]. □

Appendix B. Proof of Theorem 1

Proof. For notation convenience, we define a random variable $\xi_L := \frac{\|Y\|_2^2 - \mathbb{E}\{\|Y\|_2^2\}}{\sqrt{\mathbb{V}ar\{\|Y\|_2^2\}}} = \xi_L^1 + \xi_L^2$, where $\xi_L^i := \frac{\Delta_i - \mathbb{E}\{\Delta_i\}}{\sqrt{\mathbb{V}ar\{\|Y\|_2^2\}}}$, $i = 1, 2$. Obviously, the mean and the variance of ξ_L^i are 0 and $\frac{\mathbb{V}ar\{\Delta_i\}}{\mathbb{V}ar\{\|Y\|_2^2\}}$, respectively.

By the central limit theorem [35], we know that as $L \to \infty$

$$\xi_L^1 \xrightarrow{d} \xi^1 \sim \mathrm{N}\left(0, \frac{\mathbb{V}ar\{\Delta_1\}}{\mathbb{V}ar\{\|Y\|_2^2\}}\right) \tag{36}$$

and

$$\xi_L^2 \xrightarrow{d} \xi^2 \sim \mathrm{N}\left(0, \frac{\mathbb{V}ar\{\Delta_2\}}{\mathbb{V}ar\{\|Y\|_2^2\}}\right). \tag{37}$$

Combining (36) and (37), we have

$$\xi_L \xrightarrow{d} \xi = \xi^1 + \xi^2 \sim \mathrm{N}(0, 1), \tag{38}$$

which completes the proof of Theorem 1. □

Appendix C. Proof of Lemma 3

Proof. For any given τ_s, we can choose a detection threshold ε_0 according to (25) such that $\tilde{P}_d(\varepsilon_0, \tau_s) = \omega$. We may also choose a detection threshold $\varepsilon_1 < \varepsilon_0$ such that $\tilde{P}_d(\varepsilon_1, \tau_s) > \tilde{P}_d(\varepsilon_0, \tau_s)$ and $\tilde{P}_f(\varepsilon_1, \tau_s) > \tilde{P}_f(\varepsilon_0, \tau_s)$. In doing so, we have $F(\varepsilon_1, \tau_s) < F(\varepsilon_0, \tau_s)$. Therefore, the optimal solution to problem (33) $(\varepsilon_s^*, \tau_s^*)$ must be achieved when the equality constraint in (33a) is fulfilled, i.e., $\tilde{P}_d(\varepsilon_s^*, \tau_s^*) = \omega$. By expanding the $\tilde{P}_d(\varepsilon_s^*, \tau_s^*)$, we achieve

$$\eta(\varepsilon_s^*; L, M) = \sqrt{\mathbb{V}ar\big(\|Y\|_2^2|\mathcal{H}_1\big)}Q^{-1}(\omega) + \mathbb{E}\big(\|Y\|_2^2|\mathcal{H}_1\big), \tag{39}$$

which further completes the proof via defining $\eta(\varepsilon_s^*; L, M)$ in (13). □

Remark 3. In order to fulfill the condition (39), we could either increase ε_s (or K) at the fusion center and decrease the length of symbols sequence L at SUs, or conversely decrease ε_s (or K) and increase L. Obviously, the former one is favorable as small L saves the energy consumption of SUs. In the meanwhile, L should not be very small, otherwise the central limit theorem does not apply to (36) and (37) in Theorem 1.

Appendix D. Proof of Theorem 2

Proof. First, we take the second derivative of $\hat{F}(\tau_s)$ with respect to τ_s

$$\hat{F}''(\tau_s) = \frac{C_0 \Pr(\mathcal{H}_0)}{T}\big(2\tilde{P}_f'(\tau_s; \varepsilon_s^*) - (T - 2\tau - \tau_s)\tilde{P}_f''(\tau_s; \varepsilon_s^*)\big). \tag{40}$$

It is evident from (40) that the concavity of $\hat{F}(\tau_s)$ can be declared if $\tilde{P}_f(\tau_s; \varepsilon_s^*)$ is monotonic decreasing and convex in τ_s.

Then, taking derivative of $\tilde{P}_f(\tau_s;\varepsilon_s^*)$ with respect to τ_s yields

$$\tilde{P}_f^{'}(\tau_s;\varepsilon_s^*) = -\frac{1}{\sqrt{2\pi}}\exp\left(-\Theta^2(\tau_s)\right)\Theta^{'}(\tau_s) \tag{41}$$

with $\Theta(\tau_s) = \frac{Q^{-1}(\omega)\sqrt{A+\frac{B}{\tau_s}}+C}{\sqrt{D+\frac{E}{\tau_s}}}$, where $A = L\Omega_1(M-1+2\sigma_u^2)+L\sigma_u^4$, $B = \frac{L^2M\sigma_u^4\alpha_{arit}^2(2\gamma+1)}{2W}$, $C = LM\alpha_{arit}\gamma\sigma_u^2$, $D = L\Omega_0(M-1+2\sigma_u^2)$ and $E = \frac{L^2M\sigma_u^4\alpha_{arit}^2}{2W}$.

Further, skipping the tedious deduction we expand $\Theta^{'}(\tau_s)$ as follows

$$\Theta^{'}(\tau_s) = \underbrace{\frac{-Q^{-1}(\omega)}{2}\frac{BD-AE}{(A\tau_s+B)^{\frac{3}{2}}\sqrt{D\tau_s+E}}}_{\Phi_1(\tau_s)} + \underbrace{\frac{EC}{2\tau_s^2\left(D+\frac{E}{\tau_s}\right)^{\frac{3}{2}}}}_{\Phi_2(\tau_s)}. \tag{42}$$

It is trivial to verify that $BD-AE>0$, which together with $Q^{-1}(\omega)<0$ (as ω is close to 1) proves that $\Theta^{'}(\tau_s)>0$. Combining (41) and (42), we conclude that $\tilde{P}_f^{'}(\tau_s;\varepsilon_s^*)<0$, i.e., $\tilde{P}_f(\tau_s;\varepsilon_s^*)$ is monotonic decreasing in τ_s.

When $\varepsilon_s^*\geq\sigma_u^2$, $Q^{-1}(\omega)\sqrt{A+\frac{B}{\tau_s}}+C\geq 0$ holds and we thus have $\Theta(\tau_s)>0$. As both $\Phi_1(\tau_s)$ and $\Phi_2(\tau_s)$ are monotonic decreasing in τ_s, $\Theta^{'}(\tau_s)$ is also monotonic decreasing in τ_s. This, together with $\Theta(\tau_s)\geq 0$, implies that $\tilde{P}_f^{'}(\tau_s;\varepsilon_s^*)$ is increasing in τ_s, i.e., $\tilde{P}_f^{''}(\tau_s;\varepsilon_s^*)>0$. So far, we have proved that $\hat{F}^{''}(\tau_s)$ in (40) is negative, which implies the strict concavity of $\hat{F}(\tau_s)$ and the uniqueness of its optimal solution [36]. □

References

[1] M. Zheng, C. Xu, W. Liang, H. Yu, L. Chen, A novel coMAC-based cooperative spectrum sensing scheme in cognitive radio networks, in: Proceedings of IEEE Conference on Communications-the 7th Workshop on Cooperative and Cognitive Networks (CoCoNet7), 2015, pp. 983–987.

[2] Federal Communications Commission, Spectrum policy task force report, FCC 02–155 (2002).

[3] S. Haykin, Cognitive radio: brain-empowered wireless communications, IEEE J. Sel. Areas Commun. 23 (2) (2005) 201–220.

[4] Y. Zou, B. Champagne, W. Zhu, L. Hanzo, Relay-selection improves the security-reliability trade-off in cognitive radio systems, IEEE Trans. Commun. 63 (1) (2015) 215–228.

[5] G. Ding, Q. Wu, Y. Yao, J. Wang, Y. Chen, Kernel-based learning for statistical signal processing in cognitive radio networks: theoretical foundations, example applications, and future directions, IEEE Signal Process. Mag. 30 (4) (2013) 126–136.

[6] P. Wang, I.F. Akyildiz, On the stability of dynamic spectrum access networks in the presence of heavy tails, IEEE Trans. Wireless Commun. 14 (2) (2015) 870–881.

[7] Y.-C. Liang, Y. Zeng, E.C.Y. Peh, A.T. Hoang, Sensing-throughput tradeoff for cognitive radio networks, IEEE Trans. Wireless Commun. 7 (4) (2008) 1326–1337.

[8] T. Yucek, H. Arslan, A survey of spectrum sensing algorithms for cognitive radio applications, IEEE Commun. Surveys Tuts. 11 (1) (2009) 116–130. First Quarter.

[9] I. Sobron, P.S.R. Diniz, W.A. Martins, M. Velez, Energy detection technique for adaptive spectrum sensing, IEEE Trans. Commun. 63 (3) (2015) 617–627.

[10] E. Rebeiz, P. Urriza, D. Cabric, Optimizing wideband cyclostationary spectrum sensing under receiver impairments, IEEE Trans. on Signal Process. 61 (15) (2013) 3931–3943.

[11] E.C.Y. Peh, Y.-C. Liang, Y. Guan, Y. Zeng, Optimization of cooperative sensing in cognitive radio networks: a sensing-throughput tradeoff view, IEEE Trans. Veh. Technol. 5 (8) (2009) 5294–5299.

[12] Y. Zou, Y.D. Yao, B. Zheng, A selective-relay based cooperative spectrum sensing scheme without dedicated reporting channels in cognitive radio networks, IEEE Trans. Wireless Commun. 10 (4) (2011) 1188–1198.

[13] W. Zhang, R.K. Mallik, K.B. Lataief, Optimization of cooperative spectrum sensing with energy detection in cognitive radio networks, IEEE Trans. Wireless Commun. 8 (12) (2009) 5761–5766.

[14] Y. Chen, Optimum number of secondary users in collaborative spectrum sensing considering resources usage efficiency, IEEE Commun. Lett. 12 (December (12)) (2008) 877–879.

[15] S. Maleki, S.P. Chepuri, G. Leus, Optimization of hard fusion based spectrum sensing for energy constrained cognitive radio networks, Elsevier Phys. Commun. 9 (1) (2013) 193–198.

[16] S. Chaudhari, J. Lunden, V. Koivunen, H.V. Poor, Cooperative sensing with imperfect reporting channels: hard decisions or soft decisions? IEEE Trans. on Signal Process. 60 (1) (2012) 18–28.

[17] N. Nguyen-Thanh, P. Ciblat, S. Maleki, V.T. Nguyen, How many bits should be reported in quantized cooperative spectrum sensing? IEEE Wireless Commun. Lett. 4 (5) (2015) 465–468.

[18] Q. Zou, S. Zheng, A.H. Sayed, Cooperative sensing via sequential detection, IEEE Trans. on Signal Process. 58 (12) (2010) 6266–6283.

[19] W. Prawatmuang, D.K.C. So, E. Alsusa, Sequential cooperative sensing technique in time varying channel, IEEE Trans. Wireless Commun.. 13 (6) (2014) 3394–3405.

[20] S. Maleki, A. Pandharipande, G. Leus, Energy-efficient distributed spectrum sensing for cognitive sensor networks, IEEE Sensors J. 3 (11) (2011) 565–573.

[21] S. Maleki, G. Leus, Censored truncated sequential spectrum sensing for cognitive radio networks, IEEE J. Sel. Areas Commun. 3 (31) (2013) 364–378.

[22] S. Althunibat, F. Granelli, An objection-based collaborative spectrum sensing for cognitive radio networks, IEEE Commun. Lett. 8 (18) (2014) 1291–1294.

[23] G. Ding, J. Wang, Q. Wu, L. Zhang, Y. Zou, Y. Yao, Y. Chen, Robust spectrum sensing with crowd sensors, IEEE Trans. Commun. 62 (9) (2014) 3129–3143.

[24] H. Li, H. Dai, C. Li, Collaborative quickest spectrum sensing via random broadcast in cognitive radio systems, IEEE Trans. Wireless Commun. 9 (7) (2010) 2338–2348.

[25] G. Noh, H. Wang, J. Jo, B. Kim, D. Hong, Reporting order control for fast primary detection in cooperative spectrum sensing, IEEE Trans. Veh. Technol. 60 (8) (2011) 4058–4063.

[26] E. Axell, G. Leus, E.G. Larsson, H.V. Poor, Spectrum sensing for cognitive radio: state-of-the-art and recent advances, IEEE Signal Process. Mag. 29 (3) (2012) 101–116.

[27] S. Althunibat, M.D. Renzo, F. Granelli, Towards energy-efficient cooperative spectrum sensing for cognitive radio networks: an overview, Telecommun. Syst. 59 (1) (2015) 1–15.

[28] M. Goldenbaum, S. Stańczak, Robust analog function computation via wireless multiple-access channels, IEEE Trans. Commun. 61 (9) (2013) 3863–3876.

[29] L. Wang, K. Wu, J. Xiao, M. Hamdi, Harnessing frequency domain for cooperative sensing and multi-channel contention in CRAHNs, IEEE Trans. Wireless Commun. 13 (1) (2014) 440–449.

[30] C.H. Lim, Resource-efficient transmission for report channel in cooperative spectrum sensing, Electron. Lett. 50 (16) (2014) 1171–1173.

[31] D.A. Guimares, G.P. Aquino, M. Cattaneo, Resource efficient fusion with pre–compensated transmissions for cooperative spectrum sensing., Sensors 15 (5) (2015) 10891–10908.

[32] M. Zheng, M. Goldenbaum, S. Stańczak, H. Yu, Fast average consensus in clustered wireless sensor networks by superposition gossiping, in: Proceedings of IEEE Wireless Communication and Networking Conference, 2012, pp. 1675–1679.

[33] S. Limmer, S. Stanczak, M. Goldenbaum, R. Cavalcante, Exploiting interference for efficient distributed computation in cluster-based wireless sensor networks, in: Proceedings of IEEE Global Conference on Signal and Information Processing, 2013, pp. 933–936.

[34] M. Goldenbaum, S. Stańczak, On the channel estimation effort for analog computation over wireless multiple-access channels, IEEE Wireless Commun. Lett. 3 (3) (2014) 261–264.

[35] A.N. Shiryaev, Probability, Graduate Texts in Mathmatics, 95, 2nd, Springer, 1996.

[36] S. Boyd, L. Vandenberge, Convex Optimization, Cambridge,UK: Cambridge University Press, 2003.

[37] IEEE P802.11 task group af. Wireless LAN in the TV White Space. http://www.ieee802.org/11/Reports/tgafupdate.htm/.

Meng Zheng received the B.S. degree in information and computing science and the M.S. degree in operational research and cybernetics from Northeastern University, Shenyang, China, in 2005 and 2008, respectively, and the Ph.D. degree in mechatronic engineering from Shenyang Institute of Automation, Chinese Academy of Sciences, Shenyang, in 2012. From 2010 to 2012, he was a visiting student with the Fraunhofer Institute for Telecommunication, Heinrich Hertz Institute, Berlin, Germany. He is currently an Associate Professor with Shenyang Institute of Automation, Chinese Academy of Sciences. His research interests include wireless ad hoc and sensor networks, cognitive radio networks, and security in smart grids.

Chi Xu received the B.S. degree in communications engineering and the M.S. degree in communications and information systems from Liaoning Technical University in 2010 and 2013, respectively. He is pursuing the Ph.D. degree in control theory and control engineering at the Shenyang Institute of Automation, Chinese Academy of Sciences. His research interests include wireless sensor networks and cognitive radio networks.

Wei Liang received the Ph.D. degree in mechatronic engineering from Shenyang Institute of Automation, Chinese Academy of Sciences, Shenyang, China, in 2002. She is currently a Professor with Shenyang Institute of Automation, Chinese Academy of Sciences. As a primary participant/a project leader, she developed the WIA-PA and WIA-FA standards for industrial wireless networks, which are specified by IEC 62601 and IEC 62948, respectively. Her research interests include industrial wireless sensor networks and wireless body area networks. Dr. Liang received the International Electrotechnical Commission 1906 Award in 2015 as a distinguished expert of industrial wireless network technology and standard.

Haibin Yu received his B.S. and M.S. degrees in industrial automation from the Northeastern University, Shenyang, China, in 1984 and 1987, respectively, and Ph. D degree in control theory and control engineering from Northeastern University, Shenyang, China, in 1997. He has been with Shenyang Institute of Automation, Chinese Academy of Sciences since April 1993. He is currently a Professor and also the director of the institute. His primary research interests are in industrial communication and control systems, and industrial wireless sensor networks. In 2011, he was elected as an ISA Fellow for his contributions in industrial communication technologies. Haibin Yu has also been very active in serving professional communities. He is the Deputy Editor-in-Chief of Information and Control. He is also the Vice-Chairman of China National Technical Committee for Automation Systems and Integration Standardization, the Deputy Director of Chinese Association of Automation, the council members of China Instrument and Control Society. He is also one of the expert members for Intelligent Manufacturing Fund of the Ministry of Science and Technology of the People's Republic of China.

Lin Chen received his B.E. degree in Radio Engineering from Southeast University, China, in 2002 and the Engineer Diploma from Telecom ParisTech, Paris, in 2005. He also holds a M.S. degree of Networking from the University of Paris 6. He currently works as associate professor in the department of computer science of the University of Paris-Sud. He serves as Chair of IEEE Special Interest Group on Green and Sustainable Networking and Computing with Cognition and Cooperation, IEEE Technical Committee on Green Communications and Computing. His main research interests include modeling and control for wireless networks, distributed algorithm design and game theory.